

Published in final edited form as:

Nature. 2009 August 27; 460(7259): 1136–1139. doi:10.1038/nature08290.

## The *Ink4/Arf* locus is a barrier for iPS reprogramming

Han Li<sup>1</sup>, Manuel Collado<sup>1</sup>, Aranzazu Villasante<sup>1</sup>, Katerina Strati<sup>2</sup>, Sagrario Ortega<sup>3</sup>, Marta Cañamero<sup>4</sup>, Maria A. Blasco<sup>2</sup>, and Manuel Serrano<sup>1,\*</sup>

<sup>1</sup>Tumor Suppression Group Spanish National Cancer Research Centre (CNIO) Madrid, Spain

<sup>2</sup>Telomeres and Telomerase Group Spanish National Cancer Research Centre (CNIO) Madrid, Spain

<sup>3</sup>Transgenic Mice Unit Spanish National Cancer Research Centre (CNIO) Madrid, Spain

<sup>4</sup>Comparative Pathology Unit Spanish National Cancer Research Centre (CNIO) Madrid, Spain

### Abstract

The mechanisms involved in the reprogramming of differentiated cells into induced Pluripotent Stem (iPS) cells by Oct4, Klf4 and Sox2 (3F) remain poorly understood<sup>1</sup>. The *Ink4/Arf* tumour suppressor locus encodes three potent inhibitors of proliferation, namely p16<sup>Ink4a</sup>, p15<sup>Ink4b</sup> and Arf, which are basally expressed in differentiated cells and upregulated by aberrant mitogenic signals<sup>2-4</sup>. We show here that the locus is completely silenced in iPS cells, as well as in embryonic stem (ES) cells, acquiring the epigenetic marks of a bivalent chromatin domain, and retaining the ability to be reactivated upon differentiation. Cell culture conditions during reprogramming enhance the expression of the *Ink4/Arf* locus, further highlighting the importance of silencing the locus to allow proliferation and reprogramming. Indeed, the 3F together repress the *Ink4/Arf* locus soon after their expression and concomitant with the appearance of the first molecular markers of stemness. This downregulation also occurs in cells carrying the oncoprotein large-T, which functionally inactivates the pathways regulated by the *Ink4/Arf* locus, thus implying that the silencing of the locus is intrinsic to reprogramming and not the result of a selective process. Genetic inhibition of the *Ink4/Arf* locus has a profound positive impact on the efficiency of iPS generation, increasing both the kinetics of reprogramming and the number of emerging iPS colonies. In murine cells, Arf, rather than Ink4a, is the main barrier to reprogramming through activation of p53 and p21; whereas, in human fibroblasts, INK4a is more important than ARF. Finally, organismal aging upregulates the *Ink4/Arf* locus<sup>2,5</sup> and, accordingly, reprogramming is less efficient in cells from old organisms, but this defect can be rescued by inhibiting the locus with an shRNA. All together, we conclude that the silencing of *Ink4/Arf* locus is rate limiting for reprogramming, and its transient inhibition may significantly improve the generation of iPS.

The *Ink4/Arf* tumour suppressor locus encodes three important tumour suppressors that activate two critical anti-proliferative pathways, namely, the Rb and p53 pathways, whose activation prevents the propagation of aberrant cells, either by apoptosis or senescence (see scheme in Supplementary Fig. S1)<sup>4</sup>. Briefly, the paralogs p16<sup>Ink4a</sup> and p15<sup>Ink4b</sup> bind and inhibit the cyclin D-dependent kinases Cdk4 and Cdk6, which in turn are important to relieve the cell-cycle inhibitory activity of the Rb tumour suppressor. On the other hand, Arf

\*Correspondence: Spanish National Cancer Research Centre (CNIO) 3 Melchor Fernandez Almagro street Madrid E-28029, Spain Tel.: +34.91.732.8000 Fax: +34.91.732.8028 mserrano@cnio.es.

**Author Contributions** H.L. performed most of the experimental work. M.C. and A.V. made critical experimental contributions. K.S., S.O., and M.C. contributed experimentally. H.L., M.C., M.A.B. and M.S. designed the experimental plan, analyzed and interpreted the data. M.S. directed the project and wrote the paper.

binds and inhibits Mdm2, which is the main destabilizing enzyme of the tumour suppressor p53. Given the relevance of the *Ink4/Arf* locus in cancer protection, it is of importance to understand its behaviour upon reprogramming in relation to the “safety” of iPS cells.

We began by measuring the expression levels of the three genes encoded by the locus (*Ink4a*, *Arf*, *Ink4b*) in the parental mouse embryo fibroblasts (MEFs), in the resulting iPS after 3F-reprogramming, and in ES cells. The transcripts of the three genes of the locus were significantly repressed in iPS/ES cells compared to MEFs (Fig. 1a). In accordance with a previous report<sup>1</sup>, we observed a similar reduction in the levels of *p21* in iPS/ES cells, while the stemness markers *Nanog* and *Esg1* were abundantly expressed (Fig. 1a). To understand the epigenetic basis of the silencing of the locus in iPS/ES cells, we first examined the DNA methylation of the *Ink4a* promoter in iPS/ES cells but there was no evidence of promoter methylation (Supplementary Fig. S2). When histone marks were examined by chromatin immunoprecipitation (ChIP), we found that the repressive mark H3K9me3 essentially disappeared in ES/iPS cells compared to MEFs (Fig. 1b). In the case of the *Ink4a* promoter, the repressive mark H3K27me3 also decreased while the active mark H3K4me3 was increased (Fig. 1b). While none of the above marks by itself explains the silencing of the locus, when taken together are reminiscent of the silent chromatin configuration known as “bivalent” and characteristic of ES cells in which repressive (H3K27me3) and active (H3K4me3) marks coexist in the same molecule<sup>6-8</sup>. Bivalent chromatin has been proposed to be present at the *Ink4/Arf* locus in ES cells<sup>9</sup> and, to directly assess this, we performed sequential ChIP pulling down first H3K27me3 and then H3K4me3. We found that the *Ink4a* and *Arf* promoters are bivalent in iPS/ES cells (Fig. 1b; positive and negative controls are shown in Supplementary Fig. S3). About half of the bivalent domains in ES cells are associated to binding sites for Oct4, Sox2 or Nanog<sup>6</sup>. However, we could not detect binding of these proteins, nor of Klf4, to the three promoter regions of the *Ink4/Arf* locus (Supplementary Fig. S4). To test the functionality of the *Ink4/Arf* locus in iPS cells, we tested whether the locus is normally re-expressed upon differentiation. Addition of retinoic acid (RA) and removal of leukemia inhibitory factor (LIF)<sup>10</sup> resulted in a similar pattern of re-expression of the locus in iPS and ES cells (Fig. 1c). As another proof of the functionality of the locus, we observed re-expression of *Arf* in a teratoma spontaneously developed in an iPS-chimeric mouse (Fig. 1d). Together, these results indicate that the *Ink4/Arf* locus is epigenetically reprogrammed in iPS cells adopting a bivalent, silent, configuration and retaining its ability to be re-expressed upon differentiation or aberrant proliferation.

Culture conditions *in vitro* generally entail mitogenic hyper-stimulation, which in most primary cells results in upregulation of the *Ink4/Arf* locus<sup>11</sup>. Detailed kinetic analyses indicated that the locus is highly induced merely by the culture conditions used for reprogramming (*i.e.*, in the absence of 3F or “mock”) (Fig. 2a and b). Importantly, the upregulation of the locus is prevented by the presence of 3F, and this is clearly noticeable as soon as days 4-5 (Fig. 2b and Supplementary Fig. S5). In contrast, single factors or double combinations only partially prevented the induction of the locus (Supplementary Fig. S6). These results suggest that 3F-reprogramming inexorably includes the silencing of the *Ink4/Arf* locus. To further support this concept, we performed 3F-reprogramming in MEFs previously infected with a retrovirus expressing SV40 large-T (LT). Cells carrying LT lack functional Rb and p53 rendering the *Ink4/Arf* locus functionally irrelevant despite high levels of expression<sup>12</sup>. Interestingly, the high levels of expression of the *Ink4/Arf* locus in MEF-LT cells began to decrease soon (day 3) after introduction of 3F (Fig. 2c and Supplementary Fig. S7). These observations dissociate the silencing of the *Ink4/Arf* locus from its anti-proliferative capacity, and suggest that 3F-reprogramming, rather than selecting rare pre-existing cells with a silent *Ink4/Arf* locus, enforce a process that includes the silencing of the *Ink4/Arf* locus regardless of its functionality.

Next, we wondered whether the silencing of the *Ink4/Arf* locus was rate-limiting for reprogramming. For this, we scored the “yield” of AP-positive colonies between days 10 and 12, when colonies are first visible. The yield of colonies was corrected by the efficiency of retroviral infection measured in parallel infections with 3F plus GFP, all at equal proportions (see Methods). The efficiency of 3F reprogramming in a series (n=10) of independent wild-type MEF cultures was 0.54% (s.d.  $\pm$  0.26) (see primary data in Supplementary Table S1). Importantly, MEFs deficient in *Ink4a/Arf* were reprogrammed with an efficiency that was on average 15-fold higher than in wt MEFs (Fig. 3a and Supplementary Fig. S8). We confirmed the functionality of the *Ink4a/Arf*-null iPS by demonstrating that they are chromosomally stable (Supplementary Fig. S9), produce teratomas with representation of the three developmental layers (Supplementary Fig. S10), and generate chimeras (Supplementary Fig. S11). Deficiency of *Arf* alone also increased reprogramming efficiency by a factor of 7-fold, an effect that was quantitatively similar to that observed in *p53*-null MEFs (Fig. 3a), which is in agreement with the concept that p53 is the main target of Arf<sup>13</sup> and also with previous data indicating that p53 inhibition increases reprogramming<sup>14</sup>. The cell-cycle inhibitor p21 mediates part, but not all, the anti-proliferative effects of p53<sup>15</sup> and, interestingly reprogramming efficiency increased by a factor of 4-fold in *p21*-null MEFs (Fig. 3a). Addition of c-Myc to the reprogramming cocktail (4F-reprogramming) improved the efficiency of reprogramming of wt MEFs, and the absence of *Ink4a/Arf* still had a clear positive impact on reprogramming (Fig. 3a). To further prove the implication of *Ink4a* and *Arf* on reprogramming we performed assays on wild-type cells adding to the 3F a fourth retrovirus expressing an shRNAs against *Ink4a* (targeted to exon 1a), *Arf* (to exon 1b), or both (to the common exon 3) (see Supplementary Fig. S1). Interestingly, single inhibition of *Ink4a* or *Arf* had a beneficial effect on reprogramming, which was more prominent in the case of shArf (Fig. 3b and Supplementary Fig. S12a). Simultaneous inhibition of *Ink4a* and *Arf* had the maximal effect, close to that observed in cells genetically null for these genes (Fig. 3a and b). In agreement with the concept that retroviral vectors are only transiently expressed during reprogramming and then become permanently silenced in iPS/ES cells<sup>16</sup>, we observed that upon RA-differentiation of sh*Ink4a/Arf*-iPS cells, the levels of expression of *Ink4a* and *Arf* were normally induced (Supplementary Fig. S12b). Finally, we wanted to extend the above observations to cell types other than fibroblasts. Remarkably, when using mouse keratinocytes from newborn mice, the absence of *Ink4a/Arf* increased by more than 100-fold the yield of iPS colonies and, as in the case of MEFs, the absence of *Ink4a/Arf* had a more pronounced effect than the absence of *p53* (Fig. 3c).

In addition to the impact of the *Ink4/Arf* locus on the yield of iPS colonies, we noted that *Ink4/Arf*-null iPS colonies appear significantly faster than wt iPS colonies. For example, at day 7, wt MEFs showed “pre-iPS” micro-colonies characterized by being flat, lacking smooth borders, and having cells with a fibroblast morphology (Fig. 3e); in contrast, at this time, *Ink4a/Arf*-null MEFs already presented colonies with *bona fide* iPS/ES morphology (Fig. 3e). To further document this, we observed that the early reprogramming markers AP and SSEA1<sup>17,18</sup> appear earlier in *Ink4a/Arf*-null MEFs compared to wt MEFs, with AP being detectable as soon as day 3 (Fig. 3d). Notably, in wt MEFs, the appearance of AP and SSEA1 occurred after day 4, and this timing is contemporary to our first detectable evidence of repression of the locus by 3F (see above Fig. 2). A summary of these data is shown in Fig. 3f. The faster kinetics of reprogramming of *Ink4a/Arf*-null MEFs can be due, at least in part, to their faster proliferation rate (Supplementary Fig. S13a). However, once reprogramming is completed, both wt iPS and *Ink4a/Arf*-null iPS proliferate at similar rates (Supplementary Fig. S13b), in agreement with the fact that wt iPS have a silent *Ink4/Arf* locus. We conclude that inhibition of the *Ink4/Arf* locus has a dual impact on reprogramming, both accelerating the process and also increasing the number of successfully reprogrammed cells.

We extended the above concepts to the reprogramming of human cells. In particular, we performed 3F- and 4F-reprogramming of “telomerized” IMR90 cells, carrying ectopically expressed hTERT (IMR90/hTERT). Interestingly, supplementation of 3F or 4F with a retrovirus expressing shINK4a had a positive impact on the efficiency of reprogramming (Fig. 3g). In contrast, shARF had no impact on the reprogramming of human fibroblasts (Fig. 3g), which is in agreement with the modest role of ARF in these cells<sup>19</sup>. The human shINK4a-iPS expressed endogenous Sox2, Nanog, AP and SSEA3, and formed teratomas (Supplementary Fig. S14 and S15). When comparing the human and mouse data, it emerges a theme extensively reported in other biological contexts<sup>20</sup>, namely, that Arf dominates over Ink4a in murine cells, while INK4a dominates over ARF in human cells.

The expression of the *Ink4/Arf* locus is progressively upregulated at old ages<sup>2,5</sup>. Based on this, we hypothesized that aging should decrease reprogramming efficiency and that this should be rescued, at least in part, by inhibition of the locus. Murine skin fibroblasts (MSFs) from ear punches of old (2 years) mice had a significantly increased expression of the locus compared to MSFs from young (2 months) mice, and this was accompanied by a lower reprogramming efficiency of the old MSFs (Fig. 4a and b). Importantly, addition of shInk4a/Arf to the old MSFs rescued their low reprogramming efficiency to the same levels as young MSFs (Fig. 4b), thus suggesting that the *Ink4/Arf* locus is partly responsible for the decreased reprogramming associated to aging.

Collectively, our data indicate that the *Ink4/Arf* locus constitutes a main barrier to reprogramming in different cell types (fibroblasts and keratinocytes) and in different species (mouse and human). Experimental inhibition of the *Ink4/Arf* locus improves reprogramming efficiency, both accelerating the process and increasing the number of successfully reprogrammed cells, and transitory inhibition of the locus could be of particular practical advantage when reprogramming cells from aged individuals. Finally, recent data have pointed out similarities between malignant cells and embryonic stem cells<sup>21,22</sup> and, in this context, there is a parallelism between the known activity of *Ink4/Arf* locus as a barrier to malignancy and the new activity reported here as a barrier to de-differentiation.

## METHODS

### Culture conditions

Primary mouse embryo fibroblasts (MEFs, passage 2) and keratinocytes of the indicated genotypes were obtained from pure inbred C57BL/6 background mice, as described previously<sup>26,27</sup>. Mouse skin fibroblasts (MSFs) were obtained from the ear of young (2 months) or old (2 years) wild type C57BL/6 mice as described before<sup>28</sup>. Primary murine fibroblasts (MEFs and MSFs) were cultured in standard DMEM medium with 10% FBS (Gibco). Murine keratinocytes were cultured in basal keratinocyte media (CellnTec). Human foreskin fibroblasts IMR90 stably expressing hTERT (IMR90/hTERT) were cultured in standard DMEM medium with 10% FBS. Murine ES (mES) cells and murine iPS cells were cultured in “complete KSR medium” composed by DMEM (high glucose) supplemented with serum replacement (KSR, 15%, Invitrogen), LIF 1000 U/ml, non-essential amino acids, glutamax and beta-mercaptoethanol. C57BL/6 ES cells were derived at the Transgenic Mice Unit of the CNIO from C57BL/6 blastocysts. Human iPS (hiPS) cells were cultured in “human ES medium” composed by DMEM/F12 supplemented with serum replacement (KSR, 20%, Invitrogen), non-essential amino acids, glutamax, beta-mercaptoethanol and bFGF 4ng/ml.

### Generation of mouse iPS cells

Reprogramming of primary (passage 2-4) mouse embryo fibroblasts was performed following modifications of a previous protocol<sup>23</sup>. Briefly, retroviral supernatants were produced in HEK-293T cells ( $5 \times 10^6$  cells per 100-mm-diameter dish) transfected with the ecotropic packaging plasmid pCL-Eco (4  $\mu$ g) together with either one of the following retroviral constructs (4  $\mu$ g), pMXs-Klf4, pMXs-Sox2, pMXs-Oct4 or pMXs-cMyc (obtained from Addgene and previously described<sup>1</sup>). The retroviral vector expressing mouse shRNA against Ink4a, Arf and shInk4a/Arf, and the corresponding empty vector LMP were generously provided by Scott Lowe<sup>29</sup>. Transfections were performed using Fugene-6 transfection reagent (Roche) according to the manufacturer's protocol. Two days later, retroviral supernatants (10 ml) were collected serially during the subsequent 48 h, at 12-h intervals, each time adding fresh medium to the cells (10 ml). The recipient MEFs had been seeded the previous day ( $2.5 \times 10^5$  cells per 100-mm-diameter dish) and received 1.5 ml of each of the corresponding retroviral supernatants (amounting in the case of 3F to 4.5 ml, in the cases of 3F+shRNA or 4F to 6 ml, and in the case of 4F+shRNA to 7.5 ml). This procedure was repeated every 12 h for 2 days (a total of 4 additions). After infection was completed, media was replaced by "complete KSR medium" (see above). Cultures were maintained in the absence of drug selection with daily medium changes<sup>23</sup>. From day 10 to day 12 (according to day numbering in Fig. 2a), colonies with ES-like morphology became visible and were scored after AP staining. Colonies were picked at day 14 and expanded on feeder fibroblasts using standard procedures.

For reprogramming of murine keratinocytes, cells were freshly isolated from neonates (days 1-4 post-partum)<sup>27</sup>, and were reprogrammed at passage 5. Virus was produced in HEK-293T cells as described above, and  $3 \times 10^5$  keratinocytes were plated per 60 mm collagen-coated plate. On the two days following cell seeding, infections were performed twice daily. The keratinocytes were exposed to the cocktail of viral supernatants for one-hour intervals to prevent differentiation and then allowed to recover in basal keratinocyte media (CellNTec) between infections. The day following infection, media were changed to a "mixture medium" containing basal keratinocyte media supplemented with serum replacement (KSR, 15%, Invitrogen), LIF 1000 U/ml, non-essential amino acids, glutamax and beta-mercaptoethanol. Media was changed daily and cellular changes in plates were monitored. Clones were picked and amplified in conventional "complete KSR medium".

### Generation of human iPS cells

Reprogramming of IMR90/hTERT cells was done as previously described<sup>24,25</sup>. Briefly, retroviral supernatants were produced in HEK-293T cells ( $5 \times 10^6$  cells per 100-mm-diameter dish) transfected with the ecotropic packaging plasmid pCL-Ampho (4  $\mu$ g) together with either one of the following retroviral constructs (4  $\mu$ g), pMXs-hKlf4, pMXs-hSox2, pMXs-hOct4 and pMXs-hc-Myc (obtained from Addgene and previously described<sup>24</sup>). The retroviral vectors expressing human shRNA pRetroSuper-ARF and pRetroSuper-Ink4a were generously provided by Reuven Agami<sup>30</sup>. Transfections and infections were performed the same as mouse iPS reprogramming described above.  $2 \times 10^5$  IMR90/hTERT fibroblasts had been seeded the previous day ( $2 \times 10^5$  cells per well in 6-well gelatin-coated plates) and received 1.5 ml of each of the corresponding retroviral supernatants (either a total of three or four, as it applies, being the fourth factor the shINK4a or shARF, see later). This procedure was repeated every 12 h for 2 days (a total of 4 additions). The day after infection was completed, media was replaced, and kept for 3 additional days (days 2, 3 and 4, according to the numbering scheme in Fig. 2a). At day 5, cells were trypsinized and reseeded on feeder plates. At day 6, media was changed to "human ES medium". Cultures were maintained in the absence of drug selection with daily medium changes. At day 17, colonies with ES-like

morphology became visible at the microscope. Colonies were picked after 3 weeks and expanded on feeder fibroblasts using standard procedures.

### Reprogramming efficiency

For quantification of iPS generation efficiency, retroviral transduction was measured in parallel infections containing all the retroviruses used for reprogramming plus a GFP retrovirus (pBabe-PURO-GFP) (equal volumes of each retrovirus). Efficiency of infection was measured by FACS analysis at day 3 (see day numbering at Fig. 2a). The total number of iPS colonies was counted after staining plates for alkaline phosphatase activity (AP detection kit, Chemicon International) following the manufacturer's instructions.

### Chimera formation

The capacity of the iPS clones to generate chimeras in vivo was tested by microinjection into C57BL/6J-Tyr(C-2J)/J (albino) blastocysts, or by aggregation with CD1 (albino) morulae.

### Differentiation with retinoic acid

Differentiation with retinoic acid (RA) was performed essentially as described<sup>10</sup>. Cultures were grown to near confluency in "complete KSR medium" with LIF (day 0) and, then, trypsinized and seeded at lower density in the absence of LIF for one day (day 1). During the following two days (days 2 and 3), RA was added at a concentration of  $10^{-6}$  M.

### Teratoma formation

*Ink4/Arf*-null (3F) iPS or human iPS (4F+shINK4a or 4F+shINK4a+shARF) ( $2 \times 10^6$  cells) were subcutaneously injected into irradiated (4 Gy) nude mice (injections were performed 1 day after irradiation). Teratomas were surgically removed after 3 weeks in the case of murine iPS, or after 9 weeks in the case of human iPS. Tissue was fixed in formalin at 4°C, embedded in paraffin wax, and sectioned at a thickness of 5 µm. Sections were stained with hematoxylin and eosin for pathological examination or processed for immunohistochemical analysis with antibodies against mouse *Arf* (SantaCruz 5-C3-1) or for markers of differentiation. In the case of murine teratomas: anti-neuronal nuclei (NeuN, MAB377, Chemicon) for neuroectoderm; cytokeratin-19 (CK-19, Dev. Stu. Hybridoma Bank) for ectoderm; common-muscle actin (HHF-35, M0635, Dako) for mesoderm; and chymotrypsin (2100-0657, Serotec) for endoderm. In the case of human teratomas: synaptophysin (SY38 Dako) for ectoderm marker; smooth muscle actin (SMA 1A4 Dako) for mesoderm; and cytokeratins (AE1/AE3 Dako) for endoderm.

### Quantitative real-time PCR

Total RNAs from cells were extracted with Trizol (Life Technologies). Samples were treated with DNaseI before reverse transcription using random priming and Superscript Reverse Transcriptase (Life Technologies), according to the manufacturer's protocols. Quantitative real-time PCR was performed using an ABI PRISM 7700 (Applied Biosystems), using DNA Master SYBR Green I mix (Applied Biosystems). All values were obtained at least in duplicate and in a total of, at least, two independent assays.

The primers used were:

mInk4a-F	5'-CGTACCCCGATTTCAGGTGAT-3'
mInk4a-R	5'-TTGAGCAGAAGAGCTGCTACGT-3'
mInk4b-F	5'-AGATCCCAACGCCCTGAAC-3'
mInk4b-R	5'-CCCATCATCATGACCTGGATT-3'

mArf-F	5'-GCCGCACCGGAATCCT-3'
mArf-R	5'-TTGAGCAGAAGAGCTGCTACGT-3'
mp21-F	5'-GTGGGTCTGACTCCAGCCC-3'
mp21-R	5'-CCTTCTCGTGAGACGCTTAC-3'
mNanog-F	5'-AGGGTCTGCTACTGAGATGCTCTG-3'
mNanog-R	5'-CAACCA CTGGTTTTTCTGCCACCG-3'
mEsg1-F	5'-GAAGTCTGGTTCCTTGGCAGGATG-3'
mEsg1-R	5'-ACTCGATACACTGGCCTAGC-3'
GAPDH-F	5'-TTCACCACCATGGAGAAGGC-3'
GAPDH-R	5'-CCCTTTTGGCTCCACCCT-3'
hEndo-Sox2-F:	5'-GGGAAATGGGAGGGGTGCAAAGAGG-3'
hEndo-Sox2-R:	5'-TTGCGTGAGTGTGGATGGGATTGGTG-3'
hNanog-F:	5'-TTTCAGAGACAGAAATACCTCAGC-3'
hNanog-R:	5'-TCACACCATTGCTATTCTTCG-3'
h $\beta$ actin-F:	5'-CAAGGCCAACCGCGAGAAGAT-3'
h $\beta$ actin-R:	5'-CCAGAGGCGTACAGGGATAGCAC-3'

Calculation for the values were made using the  $\Delta\Delta C_t$  method, as previously described <sup>31</sup>.

## FACS

FACS was done as previously described <sup>17</sup>. Briefly, cells were trypsinized, washed once in PBS. For APC-conjugated SSEA1 (R&D, MC-480),  $1 \times 10^5$  cells were washed once in PBS +0.5% BSA, and incubated with 10  $\mu$ l of SSEA1 in 50  $\mu$ l of PBS+0.5% BSA for 30 min in 4°C. Afterwards, cells were washed by PBS+0.5% BSA once to remove antibody and resuspended in 300  $\mu$ l PBS for FACS analysis. For AP staining, cells were washed once in PBS and fixed/permeabilized using an intracellular staining kit (eBioscience). After permeabilization, cells were treated with 500  $\mu$ l of AP substrate (Vector Red substrate kit, Vector Laboratories) was used according to the manufacturer's protocol for 20 min. Cells were washed once and resuspended in PBS for FACS analysis. FACSCanto II (BD Biosciences) was used for all FACS analysis. Mock-infected cells were stained and analyzed in parallel to set the thresholds.

## Western blot

Cell extracts were prepared using RIPA buffer, resolved on NuPAGE 4-12% gradient Bis-Tris gels, transferred to nitrocellulose and hybridized using antibodies against Oct4 (1:250; SantaCruz H-134), Sox2 (1:250; Chemicon ab5603) and Klf4 (1:250; SantaCruz H-180).

## Immunofluorescence

MEF-LT were grown on chamber slides and infected or not with 3F following exactly the same reprogramming protocol as for the rest of the experiments. At day 3 and 8, cells were fixed with 2% paraformaldehyde for 15 min at R/T, washed with PBS and permeabilized with PBS containing 0.02% Tween-20 for 20 min. Cells were blocked in PBS with 4% BSA for 1 h and incubated with antibodies against mouse Arf (SantaCruz 5-C3-1; 1:250 in PBS +4% BSA) for 2 h, washed with PBS and further incubated with secondary anti-rat antibodies conjugated with Cy3 (1:1000 in PBS+4% BSA). For Nanog immunofluorescence of hiPS, cells were seeded in 2-well chamber slides with feeders, fixed in 4% paraformaldehyde for 15 min, permeabilized (PBS+0.1% Triton X-100) for 15 min and blocked (PBS+5% BSA) for 1 h at R/T. Nanog (1:500; Chemicon, ab5731) antibody was added and incubated in PBS+2% BSA overnight. The next day, cells were washed by PBS

and incubated with Alexa Fluor® 488 secondary antibodies against mouse (1:1000 in PBS +4% BSA). For SSEA-3 immunofluorescence of hiPS, cells were grown on 6 well plates with feeders, and fixed with 4% paraformaldehyde for 15 min at R/T. Wells were washed with PBS before blocking in PBS with 4% BSA for 1 h and incubated with antibody against human SSEA-3 (R&D, MC-631, 25 µg/ml) overnight at 4 °C. Cells were washed with PBS and further incubated with a secondary antibody as explained before for Nanog staining.

### Chromatin immunoprecipitation

Cells were crosslinked with 1% formaldehyde for 15 min at room temperature. Crosslinking was stopped by addition of glycine to a final concentration of 0.125 M. Fixed cells were lysed in lysis buffer (1% SDS, 10mM EDTA, 50 mM Tris-HCl pH8.0) and sonicated. An aliquot of 60µg was reserved as input. For immunoprecipitation, 600 µg of protein were diluted in dilution buffer (1% Triton-X100, 2mM EDTA, 150mM NaCl and 20mM Tris-HCl pH 8.0 containing protease inhibitors), and precleared with 60 µL of A/G plus-agarose (SantaCruz sc-2003). The antibodies used for the immunoprecipitation were histone H3 trimethyl Lys4 (Abcam #8580), histone H3 trimethyl Lys27 (Upstate #07-449), and histone H3 trimethyl Lys9 (Upstate #07-442). Immune complexes were precipitated with A/G plus-agarose and washed sequentially with low salt immune complex wash buffer (0.1% SDS, 1% Triton X-100, 2 mM EDTA, 20 mM Tris-HCl pH 8.1, 150 mM NaCl), high salt immune complex wash buffer (0.1% SDS, 1% Triton X-100, 2 mM EDTA, 20 mM Tris-HCl pH 8.1, 500 mM NaCl), LiCl immune complex wash buffer (0.25 M LiCl, 1% NP-40, 1% deoxycholate-Na, 1 mM EDTA, 10 mM Tris-HCl pH 8.1), and TE and then eluted in elution buffer (1% SDS, 0.1 M NaHCO<sub>3</sub>). All samples, including inputs, were de-crosslinked, treated with Proteinase K, and DNA was extracted with phenol-chloroform and resuspended in TE. Sequential ChIP experiments were carried out essentially as described above with modifications previously reported <sup>6</sup>.

The primers used for detection of promoters after ChIP were:

*mIrx2-F* 5'-TAACACGGCCTGAAATCTTCTC-3'  
*mIrx2-R* 5'-GCATCCCACTTCTACAGTCCTC-3'  
*mTcf4-F* 5'-CGGATGTGAATGGATTACAATG-3'  
*mTcf4-R* 5'-ATTGTCTCTCGGTCTGTGGT-3'  
*mInk4a-F* 5'-CAGATTGCCCTCCGATGACTTC-3'  
*mInk4a-R* 5'-TGGACCCGCACAGCAAAGAAGT-3'  
*mArf-F* 5'-GCCTCGCCGATCTTCTATTTTCT-3'  
*mArf-R* 5'-CCCATCGCGGTGACAGC-3'  
*mInk4b-F* 5'-ACCAAGCGAAGGAACATACTGC-3'  
*mInk4b-R* 5'-GGCACCTGGCTTCTTTAAGA-3'

### Supplementary Material

Refer to Web version on PubMed Central for supplementary material.

### Acknowledgments

We thank Scott Lowe and Reuven Agami for reagents. We are indebted to Maribel Muñoz, Orlando Dominguez, Diego Megias and Helia Schonthaler. H.L. is recipient of a "Juan de la Cierva" contract from the Spanish Ministry of Science (MICINN). M.C. is recipient of a "Ramon y Cajal" contract (MICINN). Work in the laboratory of M.S. is funded by the CNIO and by grants from the MICINN (SAF and CONSOLIDER), the Regional Government of Madrid, the European Union, the European Research Council (ERC), and the "Marcelino Botin" Foundation.



## REFERNECES

1. Takahashi K, Yamanaka S. Induction of pluripotent stem cells from mouse embryonic and adult fibroblast cultures by defined factors. *Cell*. 2006; 126:663–676. [PubMed: 16904174]
2. Collado M, Blasco MA, Serrano M. Cellular senescence in cancer and aging. *Cell*. 2007; 130:223–233. [PubMed: 17662938]
3. Serrano M, Lin AW, McCurrach ME, Beach D, Lowe SW. Oncogenic ras provokes premature cell senescence associated with accumulation of p53 and p16INK4a. *Cell*. 1997; 88:593–602. [PubMed: 9054499]
4. Sharpless NE. INK4a/ARF: a multifunctional tumor suppressor locus. *Mutat Res*. 2005; 576:22–38. [PubMed: 15878778]
5. Krishnamurthy J, et al. Ink4a/Arf expression is a biomarker of aging. *J Clin Invest*. 2004; 114:1299–1307. [PubMed: 15520862]
6. Bernstein BE, et al. A bivalent chromatin structure marks key developmental genes in embryonic stem cells. *Cell*. 2006; 125:315–326. [PubMed: 16630819]
7. Azuara V, et al. Chromatin signatures of pluripotent cell lines. *Nat Cell Biol*. 2006; 8:532–538. [PubMed: 16570078]
8. Mikkelsen TS, et al. Genome-wide maps of chromatin state in pluripotent and lineage-committed cells. *Nature*. 2007; 448:553–560. [PubMed: 17603471]
9. Ohm JE, et al. A stem cell-like chromatin pattern may predispose tumor suppressor genes to DNA hypermethylation and heritable silencing. *Nat Genet*. 2007; 39:237–242. [PubMed: 17211412]
10. Savatier P, Lapillonne H, van Grunsven LA, Rudkin BB, Samarut J. Withdrawal of differentiation inhibitory activity/leukemia inhibitory factor up-regulates D-type cyclins and cyclin-dependent kinase inhibitors in mouse embryonic stem cells. *Oncogene*. 1996; 12:309–322. [PubMed: 8570208]
11. Sharpless NE. Ink4a/Arf links senescence and aging. *Exp Gerontol*. 2004; 39:1751–1759. [PubMed: 15582292]
12. Hara E, et al. Regulation of p16CDKN2 expression and its implications for cell immortalization and senescence. *Mol Cell Biol*. 1996; 16:859–867. [PubMed: 8622687]
13. Sherr CJ. Divorcing ARF and p53: an unsettled case. *Nat Rev Cancer*. 2006; 6:663–673. [PubMed: 16915296]
14. Zhao Y, et al. Two supporting factors greatly improve the efficiency of human iPSC generation. *Cell Stem Cell*. 2008; 3:475–479. [PubMed: 18983962]
15. Sherr CJ, Roberts JM. CDK inhibitors: positive and negative regulators of G1-phase progression. *Genes Dev*. 1999; 13:1501–1512. [PubMed: 10385618]
16. Cherry SR, Biniszkiwicz D, van Parijs L, Baltimore D, Jaenisch R. Retroviral expression in embryonic stem cells and hematopoietic stem cells. *Mol Cell Biol*. 2000; 20:7419–7426. [PubMed: 11003639]
17. Brambrink T, et al. Sequential expression of pluripotency markers during direct reprogramming of mouse somatic cells. *Cell Stem Cell*. 2008; 2:151–159. [PubMed: 18371436]
18. Stadtfeld M, Maherali N, Breault DT, Hochedlinger K. Defining molecular cornerstones during fibroblast to iPSC cell reprogramming in mouse. *Cell Stem Cell*. 2008; 2:230–240. [PubMed: 18371448]
19. Wei W, Hemmer RM, Sedivy JM. Role of p14(ARF) in replicative and induced senescence of human fibroblasts. *Mol Cell Biol*. 2001; 21:6748–6757. [PubMed: 11564860]
20. Evan GI, d'Adda di Fagagna F. Cellular senescence: hot or what? *Curr Opin Genet Dev*. 2009; 19:25–31. [PubMed: 19181515]
21. Wong DJ, et al. Module map of stem cell genes guides creation of epithelial cancer stem cells. *Cell Stem Cell*. 2008; 2:333–344. [PubMed: 18397753]
22. Ben-Porath I, et al. An embryonic stem cell-like gene expression signature in poorly differentiated aggressive human tumors. *Nat Genet*. 2008; 40:499–507. [PubMed: 18443585]
23. Blelloch R, Venere M, Yen J, Ramalho-Santos M. Generation of induced pluripotent stem cells in the absence of drug selection. *Cell Stem Cell*. 2007; 1:245–247. [PubMed: 18371358]

24. Takahashi K, et al. Induction of pluripotent stem cells from adult human fibroblasts by defined factors. *Cell*. 2007; 131:861–872. [PubMed: 18035408]
25. Park IH, et al. Reprogramming of human somatic cells to pluripotency with defined factors. *Nature*. 2008; 451:141–146. [PubMed: 18157115]
26. Palmero I, Serrano M. Induction of senescence by oncogenic Ras. *Methods Enzymol*. 2001; 333:247–256. [PubMed: 11400340]
27. Munoz P, Blanco R, Flores JM, Blasco MA. XPF nuclease-dependent telomere loss and increased DNA damage in mice overexpressing TRF2 result in premature aging and cancer. *Nat Genet*. 2005; 37:1063–1071. [PubMed: 16142233]
28. Li H, Vogel H, Holcomb VB, Gu Y, Hastay P. Deletion of Ku70, Ku80, or both causes early aging without substantially increased cancer. *Mol Cell Biol*. 2007; 27:8205–8214. [PubMed: 17875923]
29. Dickins RA, et al. Probing tumor phenotypes using stable and regulated synthetic microRNA precursors. *Nat Genet*. 2005; 37:1289–1295. [PubMed: 16200064]
30. Voorhoeve PM, Agami R. The tumor-suppressive functions of the human INK4A locus. *Cancer Cell*. 2003; 4:311–319. [PubMed: 14585358]
31. Yuan JS, Reed A, Chen F, Stewart CN Jr. Statistical analysis of real-time PCR data. *BMC Bioinformatics*. 2006; 7:85. [PubMed: 16504059]

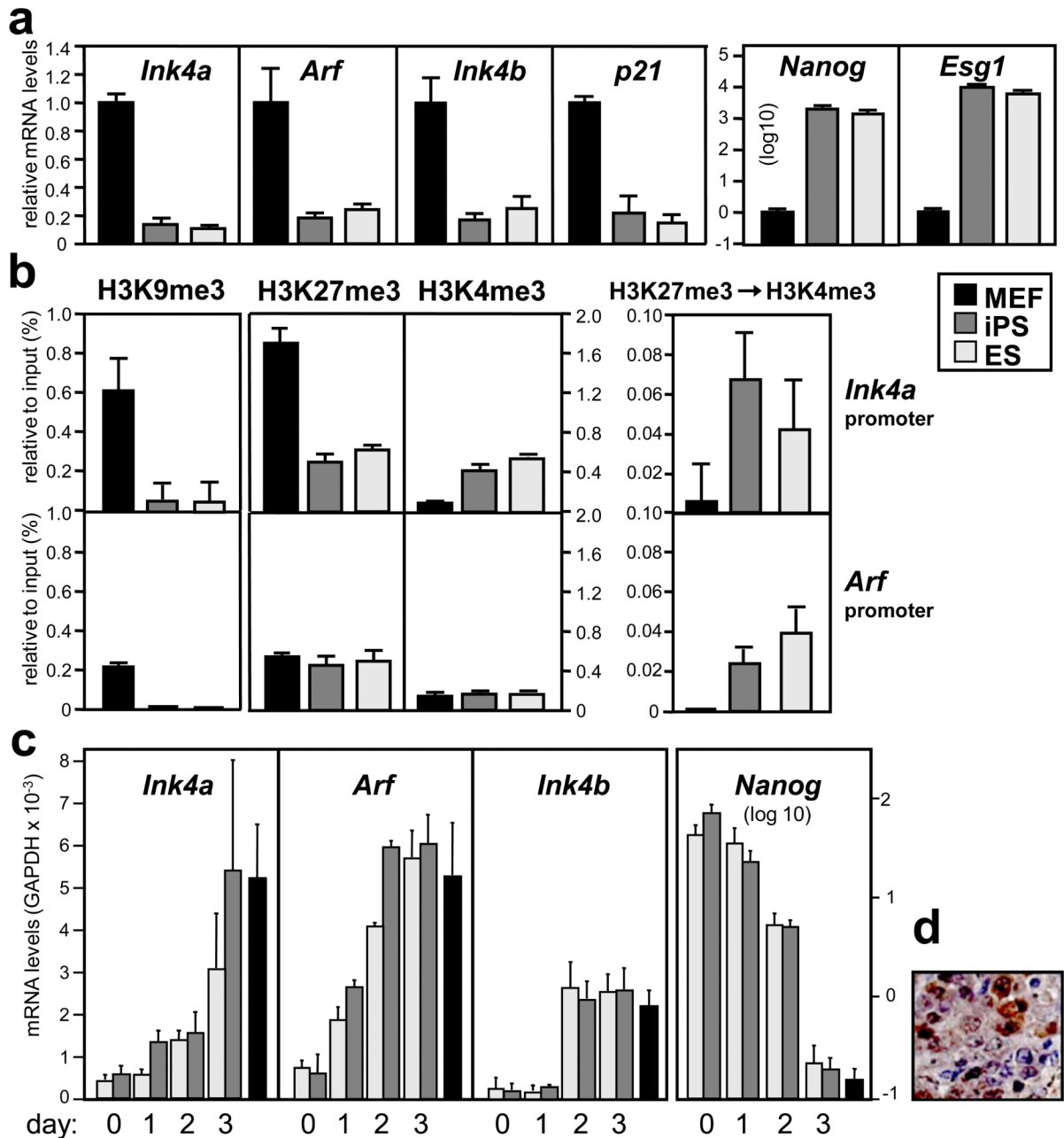


### Figure 1. Functional reprogramming of the *Ink4/Arf* locus

**a.** Expression of the indicated genes in iPS compared with their parental MEFs and with ES cells measured by quantitative RT-PCR. **b.** Epigenetic marks present at the indicated promoters. Sequential ChIP, first of H3K27me3 and then of H3K4me3, is in the leftmost panel. Data correspond to the average  $\pm$  s.d. of a representative assay from at least 2 independent assays. **c.** Expression of the indicated genes in iPS and in ES cells undergoing differentiation by addition of retinoic acid in the absence of LIF. Data correspond to the average  $\pm$  s.d. of at least 2 independent assays. **d.** Re-expression of *Arf* in a teratoma developed in a chimeric-iPS mouse detected by immunohistochemistry.

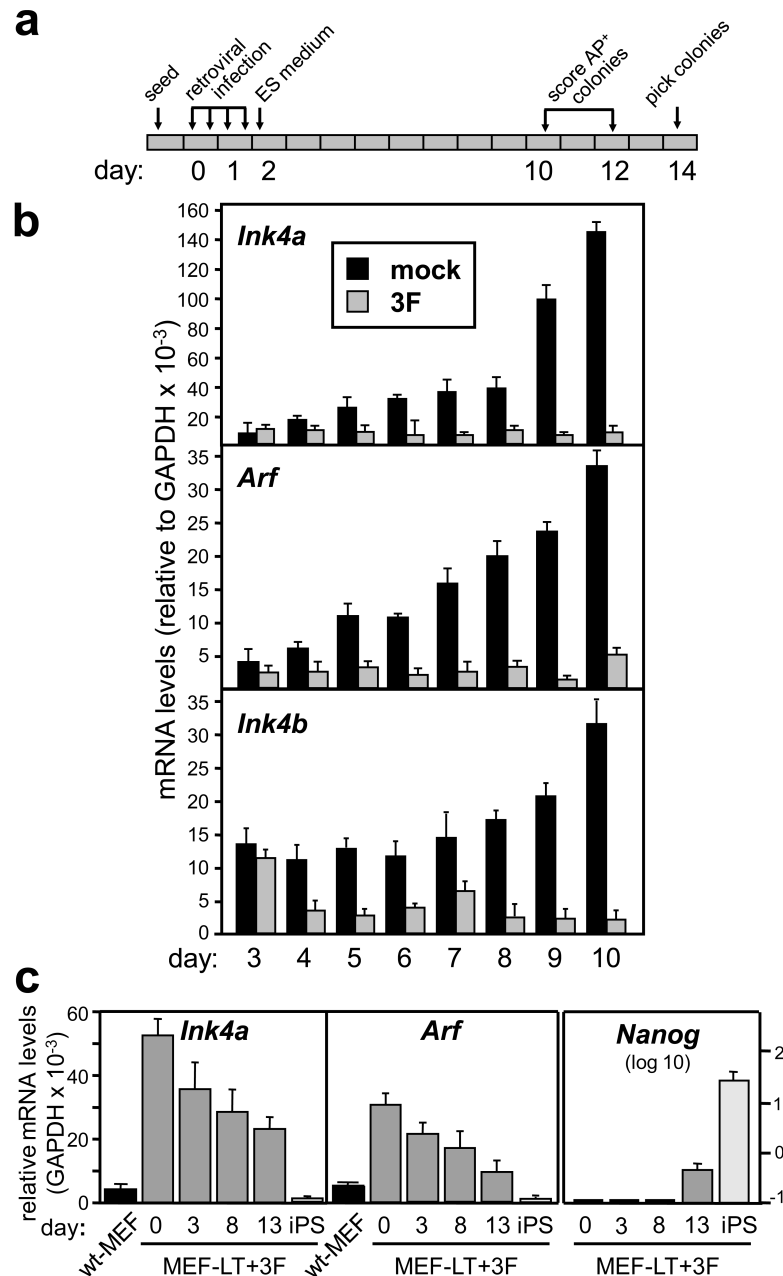


**Figure 2. Silencing of the *Ink4/Arf* locus during reprogramming**

**a.** Experimental layout and day numbering. **b.** Kinetics of expression of the *Ink4/Arf* locus in mock-infected (mock) and 3F-infected (3F) MEFs, measured by quantitative RT-PCR. **c.** Repression of *Ink4a* and *Arf* during 3F-reprogramming of MEFs expressing large-T (MEF-LT+3F), measured by qRT-PCR. Data correspond to the average  $\pm$  s.d. of at least 2 independent assays.

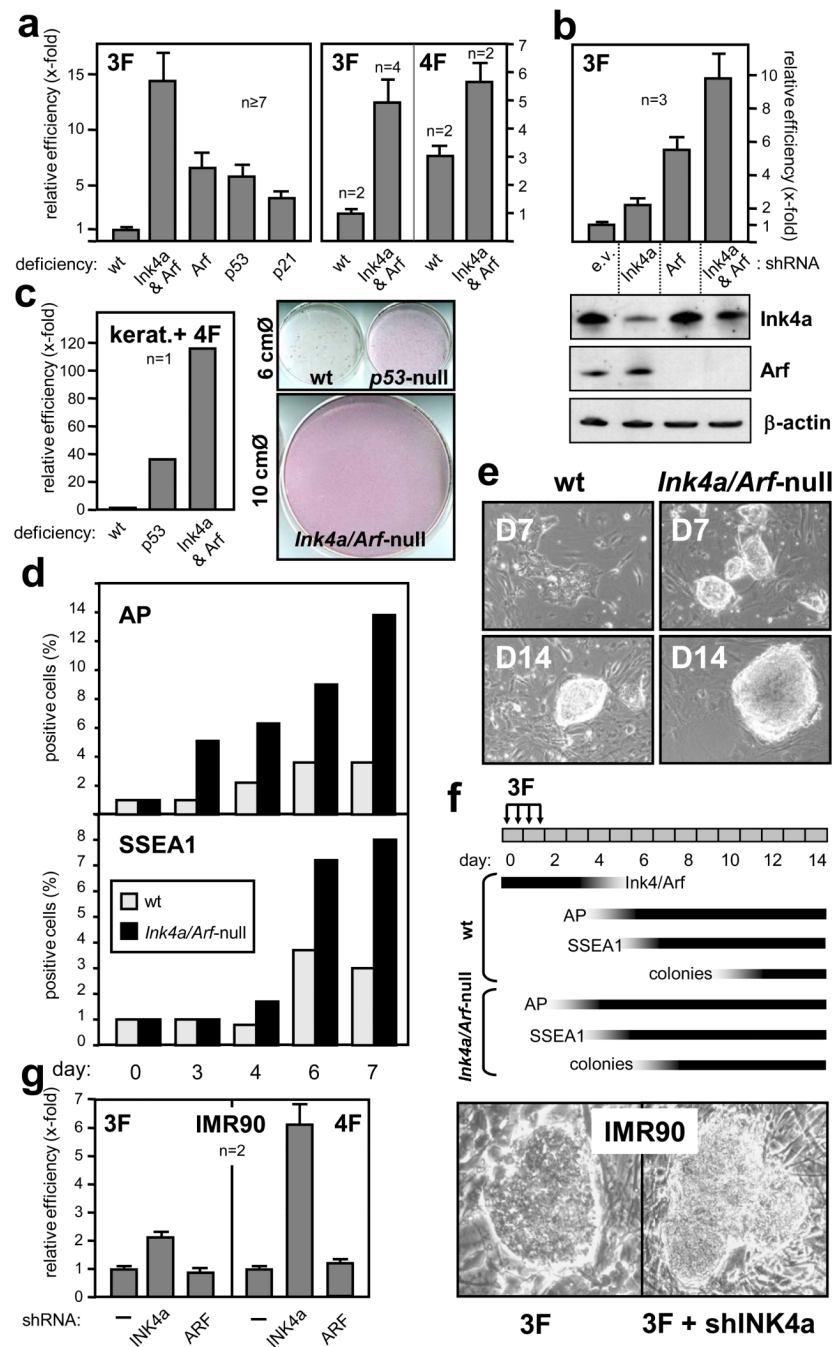


### Figure 3. Impact of *Ink4a/Arf* on reprogramming efficiency

**a.** Reprogramming efficiencies of MEFs of the indicated genotypes relative to wt MEFs. Data correspond to the average  $\pm$  s.e.m.; n, independent assays with different MEF isolates. **b.** Fold change of reprogramming efficiency of primary wt MEFs retrovirally infected with 3F plus empty vector (e.v.) or the indicated shRNAs. Data correspond to the average  $\pm$  s.d. Protein levels were analyzed 48 h after infection. **c.** Fold change of reprogramming efficiency measured in newborn keratinocytes of the indicated genotypes. **d.** Kinetics of expression of pluripotency markers AP and SSEA1 during 3F-reprogramming, measured by FACS. **e.** Representative images of colonies at days 7 and 14. **f.** Schematic representation of

the kinetics of *Ink4/Arf* locus suppression and marker expression during reprogramming. **g.** Reprogramming efficiencies of human diploid fibroblasts IMR90/hTERT using 3F or 4F plus the indicated shRNAs. Data correspond to the average  $\pm$  s.d. The right panels show representative iPS colonies.

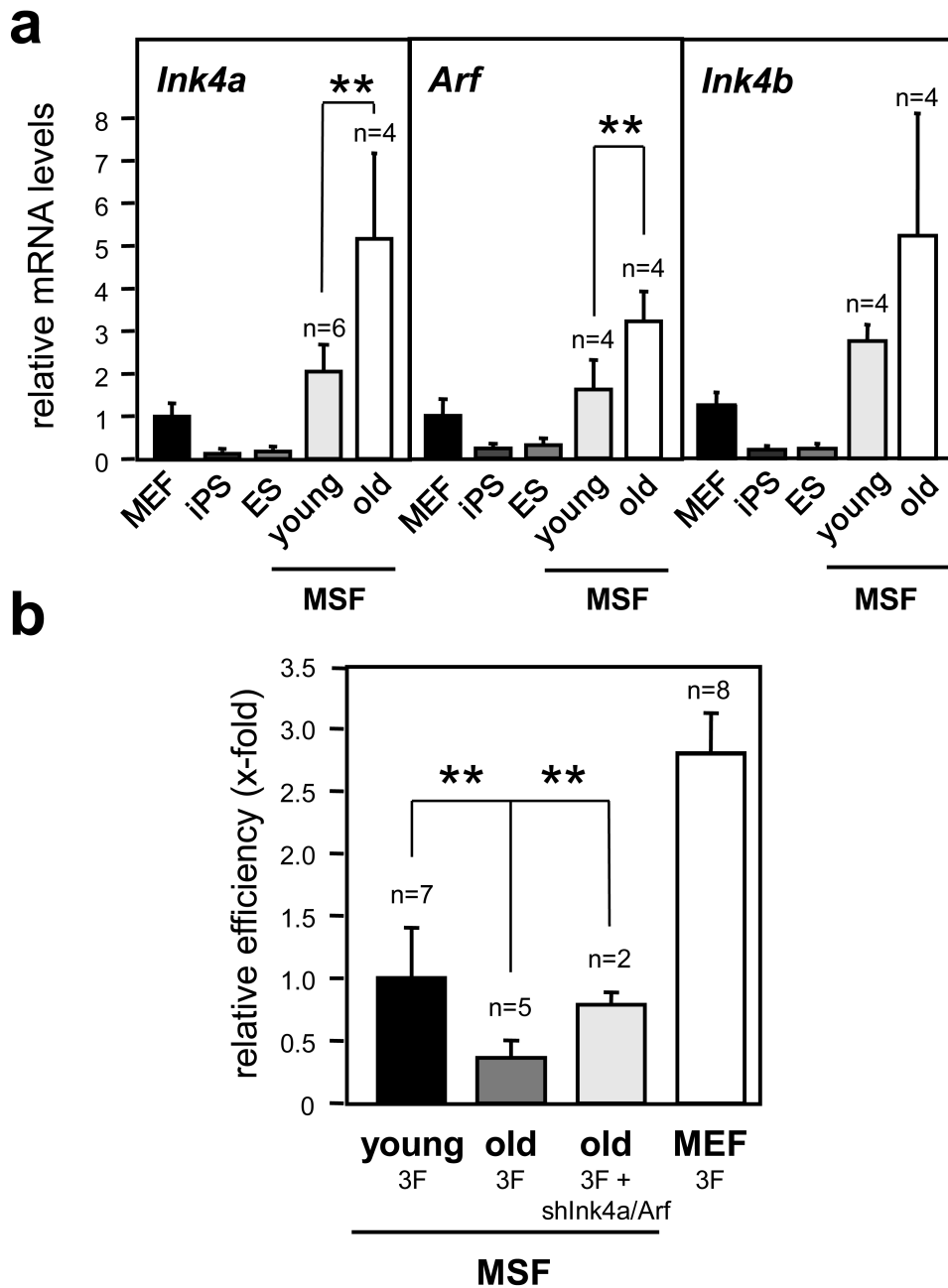


**Figure 4. Association between age of the parental cells, expression of the *Ink4/Arf* locus and reprogramming efficiency**

**a.** Expression of the *Ink4/Arf* locus in mouse skin fibroblasts (MSF) from 2-month old (young) or 2-year old (old) mice, compared to MEF, iPS and ES cells, measured by qRT-PCR. **b.** Reprogramming efficiencies of old MSFs by 3F plus or minus shInk4a/Arf. Data correspond to the average  $\pm$  s.d. Statistical significance: \*\* $p < 0.01$ .